

## Supporting Information for:

# Ring-opening polymerization of $\epsilon$ -caprolactone by lithium piperazinyl-aminephenolate complexes: Synthesis, characterization and kinetic studies

Nduka Ikpo,<sup>a</sup> Christian Hoffmann,<sup>a</sup> Louise N. Dawe,<sup>ab</sup> and Francesca M. Kerton<sup>\*a</sup>

Department of Chemistry, Memorial University of Newfoundland, St. John's, Newfoundland, Canada A1B 3X7

## Contents

Variable temperature NMR spectrum of the methylene region of <b>3</b> in C <sub>5</sub> D <sub>5</sub> N	<b>Fig. S1</b>
Effect of monomer concentration on the time of polymer conversion initiated by <b>1</b>	<b>Fig. S2</b>
Semilogarithmic plots of ln[CL] <sub>0</sub> /[CL] <sub>t</sub> versus time for the polymerization initiated by <b>3</b> at various temperatures	<b>Fig. S3</b>
Arrhenius plots of ln <i>k<sub>p</sub></i> vs. 1/T for the ROP of $\epsilon$ -CL initiated by <b>3</b>	<b>Fig. S4</b>
Semilogarithmic plots of ln[CL] <sub>0</sub> /[CL] <sub>t</sub> versus time for the polymerization initiated by <b>3</b> -BnOH at various temperatures	<b>Fig. S5</b>
Arrhenius plots of ln <i>k<sub>p</sub></i> vs. 1/T for the ROP of $\epsilon$ -CL initiated by <b>3</b> -BnOH	<b>Fig. S6</b>
<sup>13</sup> C NMR spectra for PCL initiated by (a) <b>3</b> and (b) <b>2</b> -BnOH	<b>Fig. S7</b>
MALDI-TOF mass spectrum of PCL initiated by <b>1</b> in THF at 60 °C	<b>Fig. S8</b>
MALDI-TOF mass spectrum of PCL initiated by <b>1</b> in toluene at 25 °C	<b>Fig. S9</b>
MALDI-TOF mass spectrum of PCL initiated by <b>1</b> -BnOH in toluene at 25 °C	<b>Fig. S10</b>
MALDI-TOF mass spectrum of PCL initiated by <b>1</b> -BnOH in toluene at 60 °C	<b>Fig. S11</b>
MALDI-TOF mass spectrum of PCL initiated by <b>3</b> -BnOH in toluene at 25 °C	<b>Fig. S12</b>
MALDI-TOF mass spectrum of PCL initiated by <b>3</b> -BnOH in toluene at 40 °C	<b>Fig. S13</b>
Molecular structure of <b>3</b> .	<b>Fig. S14</b>

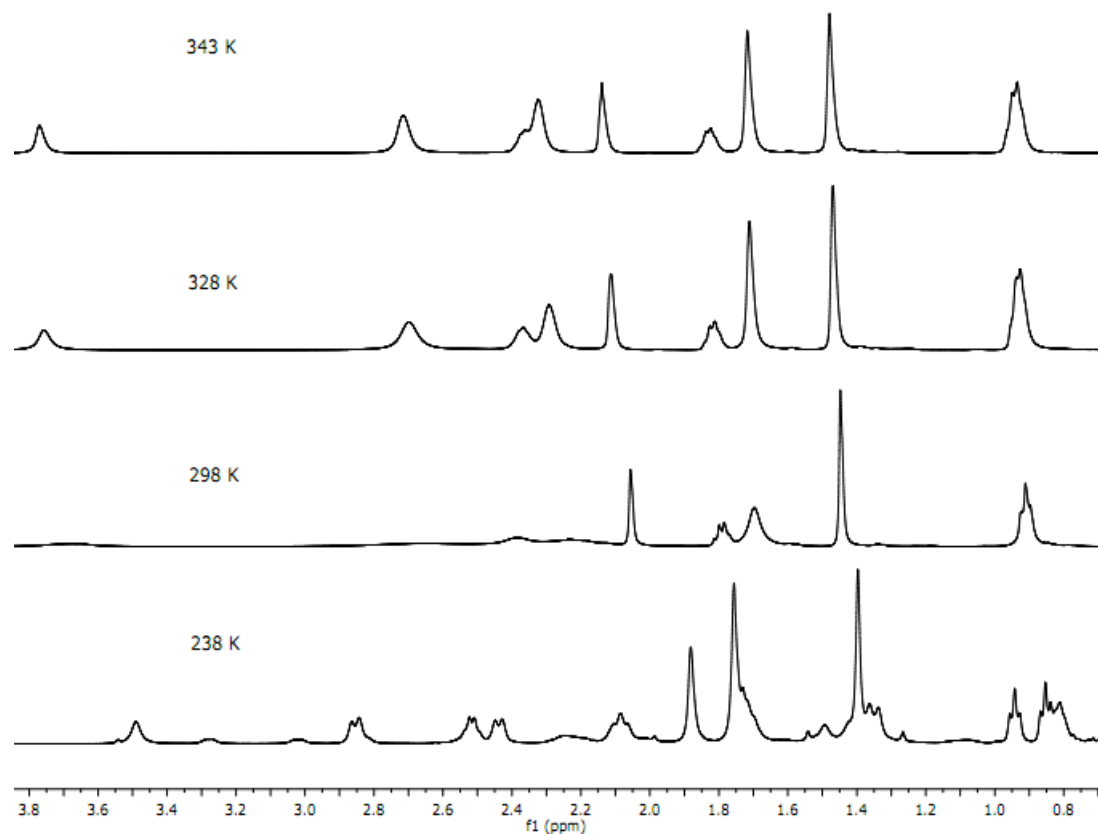


**Fig. S1** Variable temperature NMR spectrum of the methylene region of **3** in C<sub>5</sub>D<sub>5</sub>N.

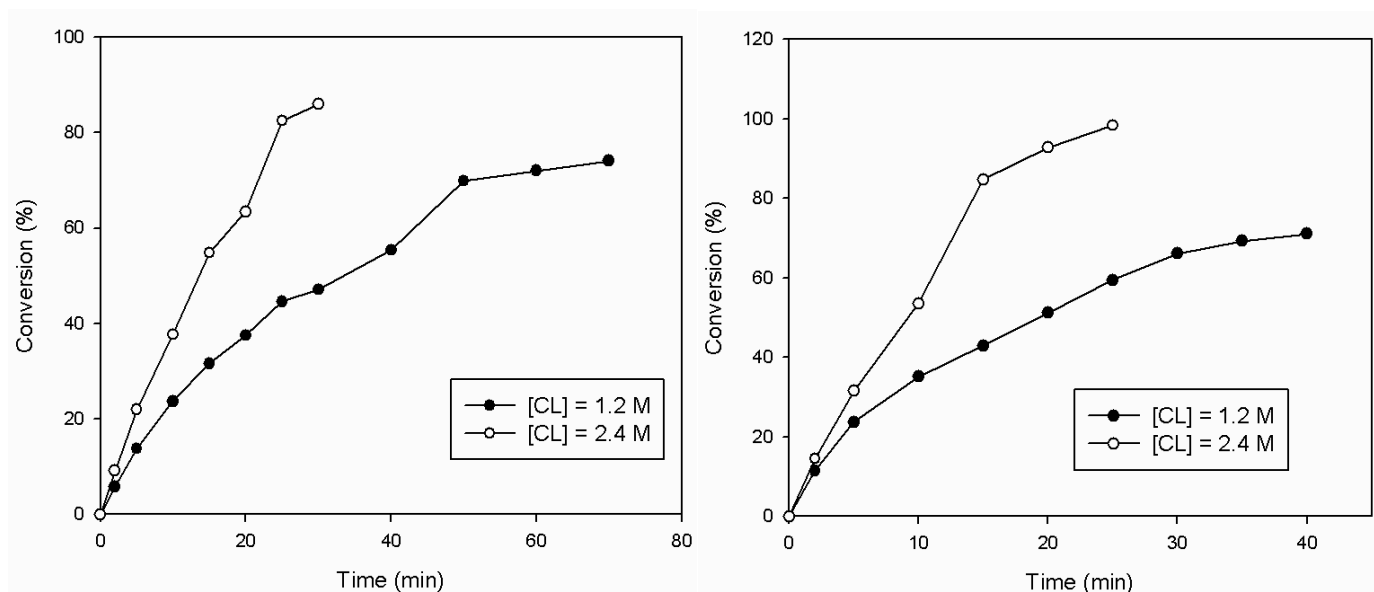


**Fig. S2:** Effect of monomer concentration on the time of polymer conversion. {Conditions: **[1]** = 17.7 mM in toluene; [CL] = 1.2 (●); [CL] = 2.4 M (○)} at (a) 40 °C and (b) 60 °C

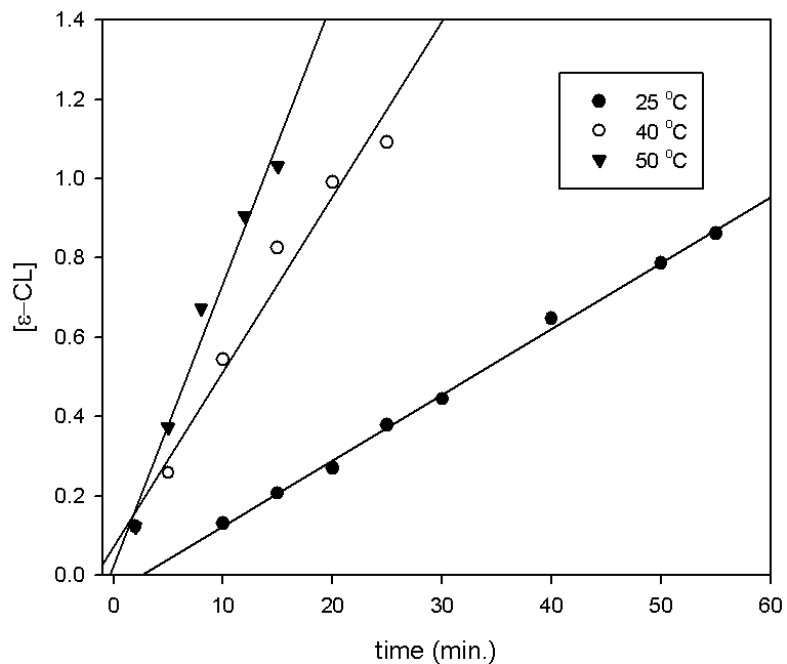


**Fig. S3:** Semilogarithmic plots of the monomer conversion stated as  $\ln[\text{CL}]_0/[\text{CL}]_t$  versus the reaction time for the polymerization of  $\varepsilon$ -caprolactone at different temperatures initiated with **3**;  $[\text{CL}]_0/[\mathbf{3}]_0 = 200$ , ( $[1]_0 = 17.7$  mM,  $[\text{CL}] = 1.52$  M); (●) = 25 °C, (○) = 40 °C, (▼) = 50 °C.

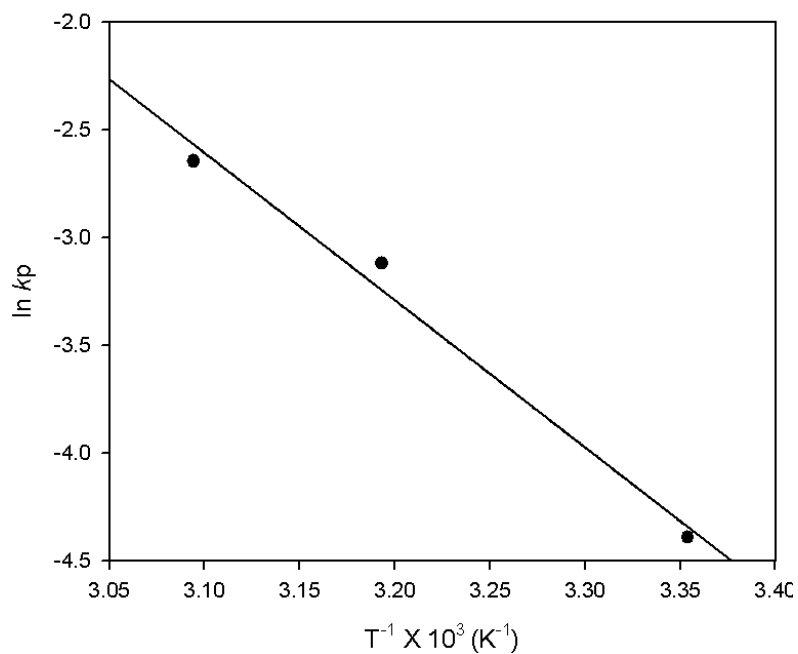


**Fig. S4:** Arrhenius plots of  $\ln(kp)$  vs.  $1/T$  for the ring-opening polymerization of  $\varepsilon$ -caprolactone initiated by **3**: $[\mathbf{3}] = 17.7$  mM;  $[\text{CL}]/[1] = 200$

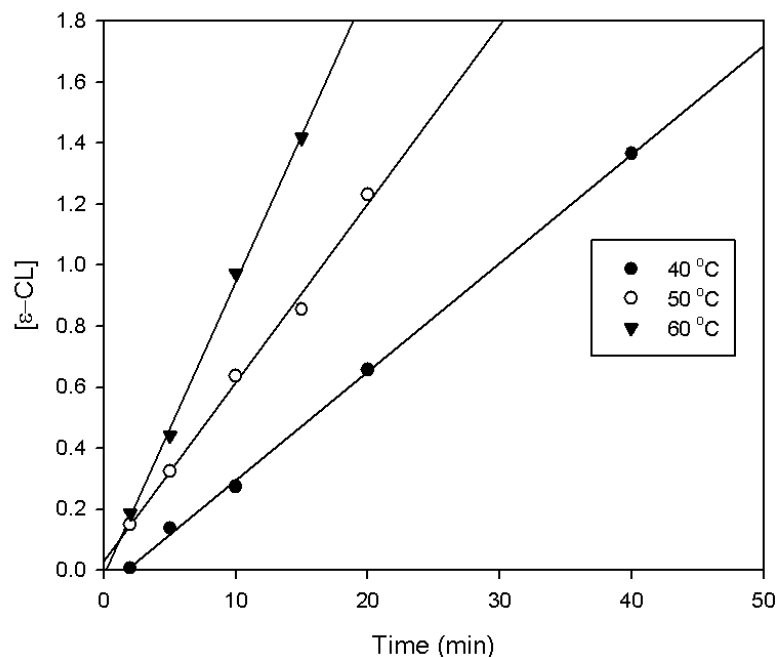


**Fig. S5:** Semilogarithmic plots of the monomer conversion stated as  $\ln[\text{CL}]_0/[\text{CL}]_t$  versus the reaction time for the polymerization of  $\varepsilon$ -caprolactone at different temperatures initiated with **3**-BnOH;  $[\text{CL}]_0/[\mathbf{3}\text{-BnOH}]_0 = 200$ , ( $[1]_0 = 17.7$  mM,  $[\text{CL}] = 1.52$  M); (●) = 40 °C, (○) = 50 °C, (▼) = 60 °C.

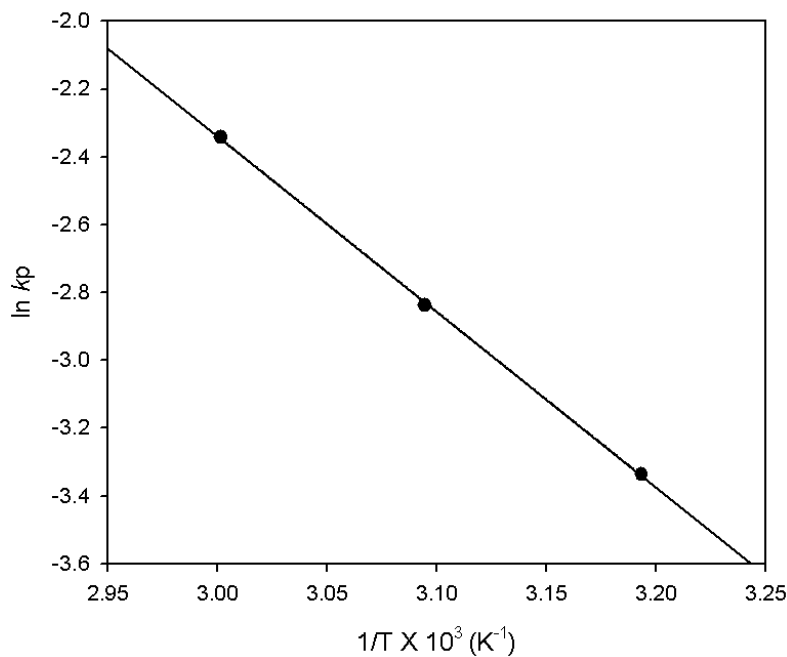


**Fig. S6:** Arrhenius plots of  $\ln(k_p)$  vs.  $1/T$  for the ring-opening polymerization of  $\varepsilon$ -caprolactone initiated by **3**: $[\mathbf{3}\text{-BnOH}] = 17.7$  mM;  $[\text{CL}]/[1] = 200$

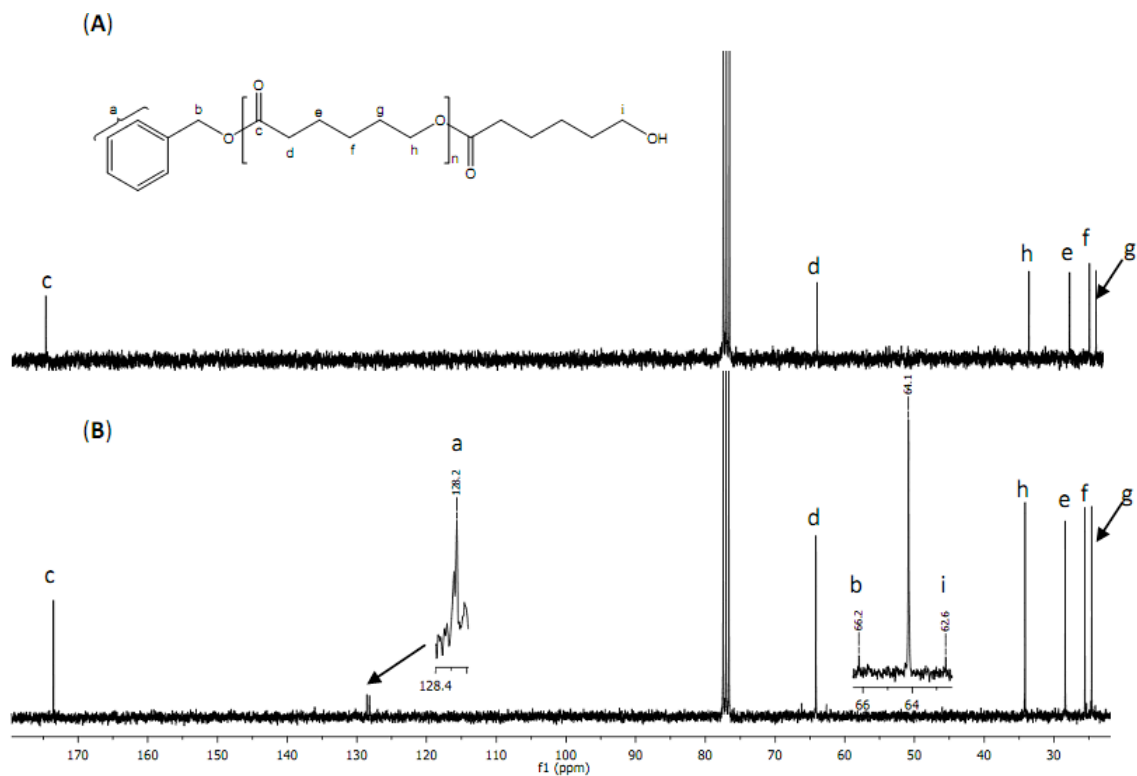


**Fig. S7:**  $^{13}\text{C}$  NMR spectra for PCL initiated by (A) **3** and (B) **2-BnOH** (Table 1, entry 18 and 15).

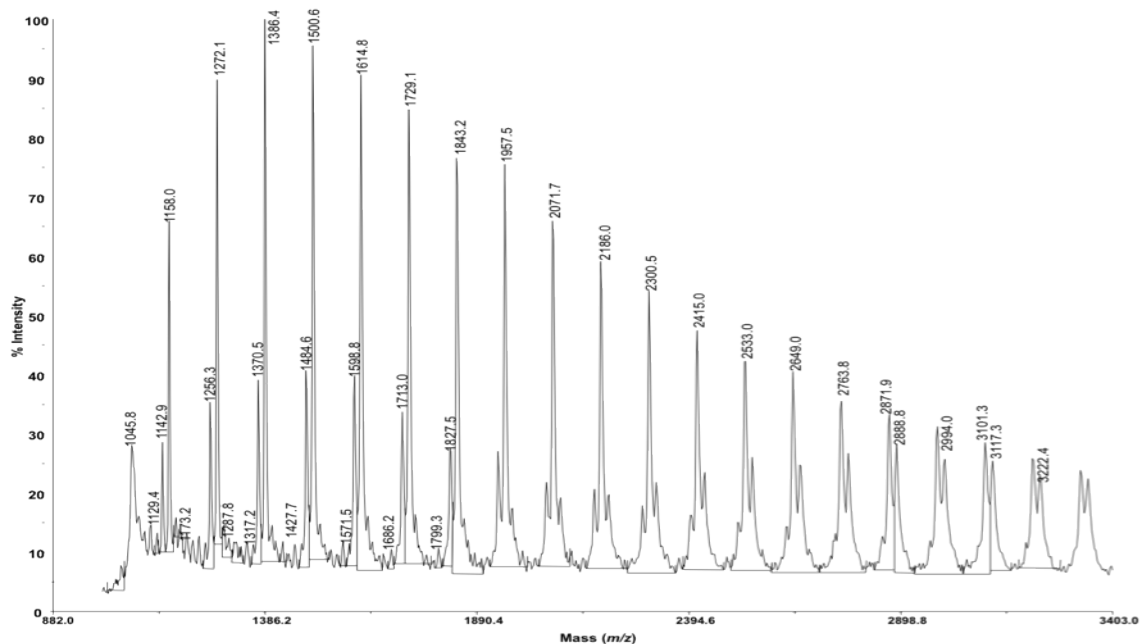


**Fig. S8** MALDI-TOF mass spectrum of PCL initiated by **1** in THF at 60 °C,  $[\text{CL}]/[\mathbf{1}] = 50$  (Table 1, entry 2). The absolute mass values meet the data of  $114.14 \times n$  for  $(\text{CL})_n$ ,  $114.14 \times n + 17$  for  $\text{H}-(\text{CL})_n-\text{OH}$ ,  $114.14 \times n + 17 + 22$  for  $\text{H}-(\text{CL})_n-\text{OH} \cdot \text{Na}^+$  and  $114.14 \times n + 17 + 22$  for  $\text{H}-(\text{CL})_n-\text{OH} \cdot \text{K}^+$ .

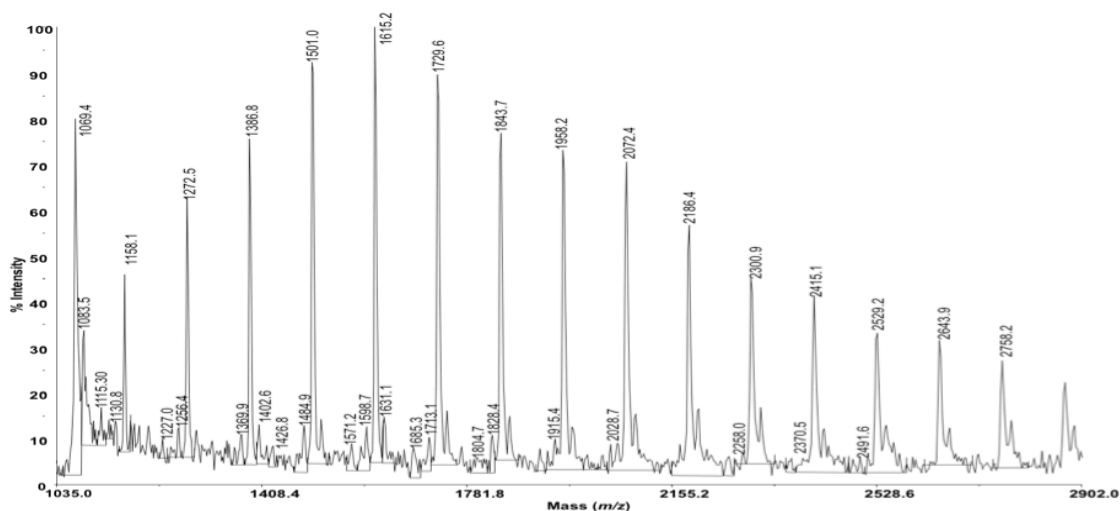


**Fig. S9** MALDI-TOF mass spectrum of PCL initiated by **1** in toluene at 25 °C, [CL]/[**1**] = 50 (Table 1, entry 5). The absolute mass values meet the data of  $114.14 \times n$  for  $(\text{CL})_n$ ,  $114.14 \times n + 17$  for  $\text{H}-(\text{CL})_n-\text{OH}$ ,  $114.14 \times n + 17 + 22$  for  $\text{H}-(\text{CL})_n-\text{OH} \cdot \text{Na}^+$  and  $114.14 \times n + 17 + 22$  for  $\text{H}-(\text{CL})_n-\text{OH} \cdot \text{K}^+$ .

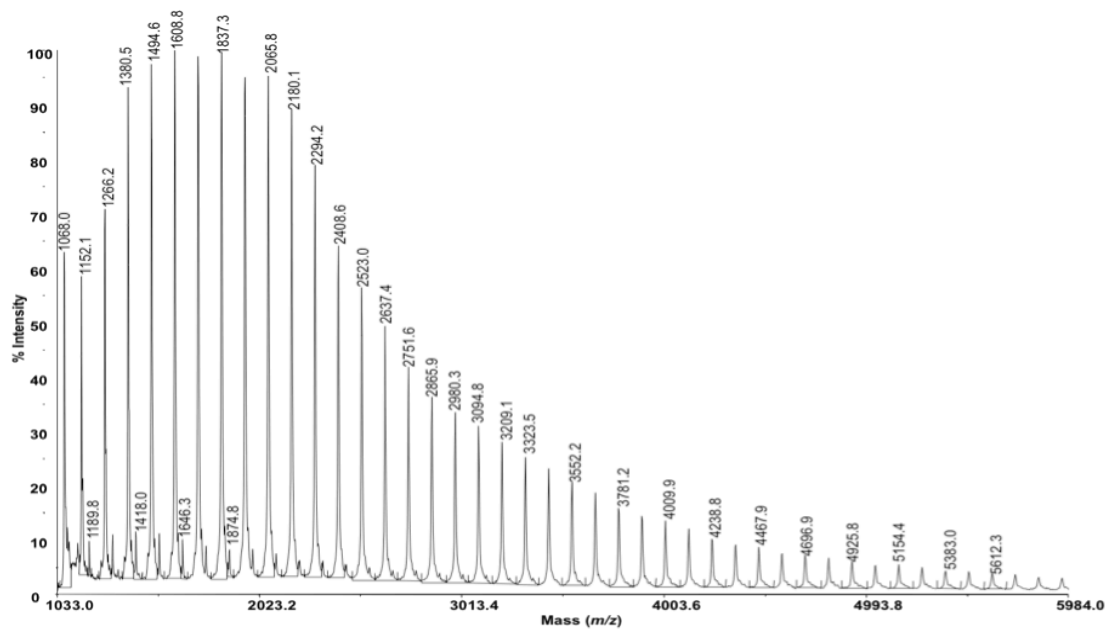


**Fig. S10** MALDI-TOF mass spectrum of PCL initiated by **1-BnOH** in toluene at 25 °C, [CL]/[**1-BnOH**] = 50 (Table 1, entry 9). The absolute mass values meet the data of  $114.14 \times n + 108$  for  $\text{BnO}-(\text{CL})_n-\text{H}$ ,  $114.14 \times n + 108 + 17$  for  $\text{BnO}-(\text{CL})_n-\text{OH}$  and  $114.14 \times n + 108 + 17 + 22$  for  $\text{BnO}-(\text{CL})_n-\text{OH} \cdot \text{K}^+$ .

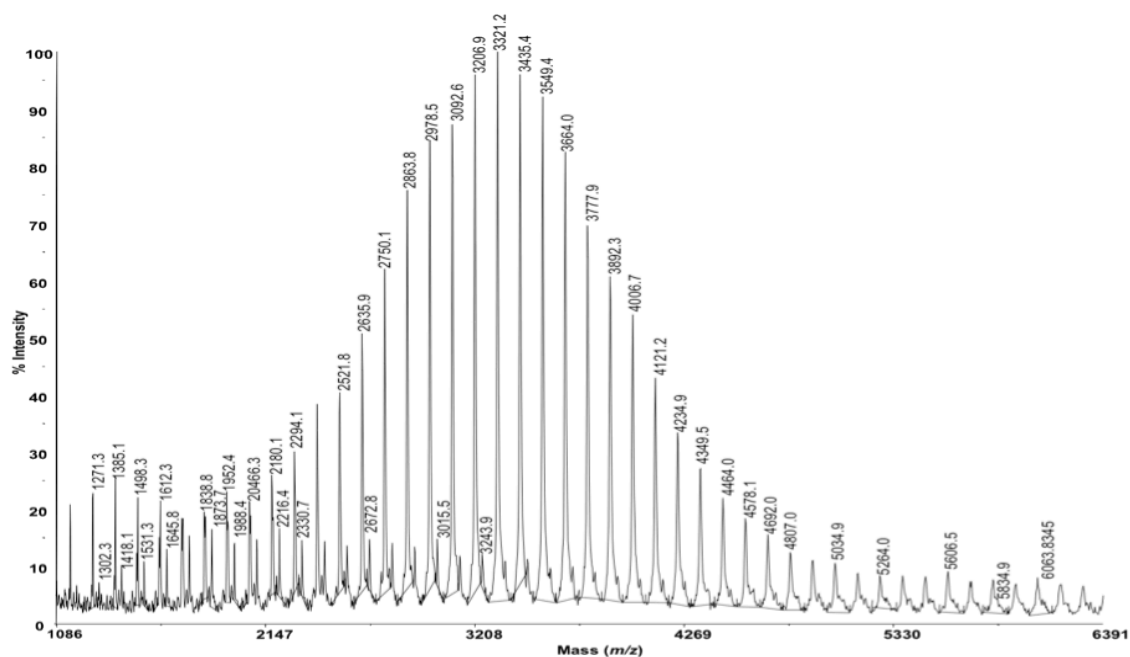


**Fig. S11** MALDI-TOF mass spectrum of PCL initiated by **1**-BnOH in toluene at 60 °C, [CL]/[**1**-BnOH] = 200 (Table 1, entry 12).

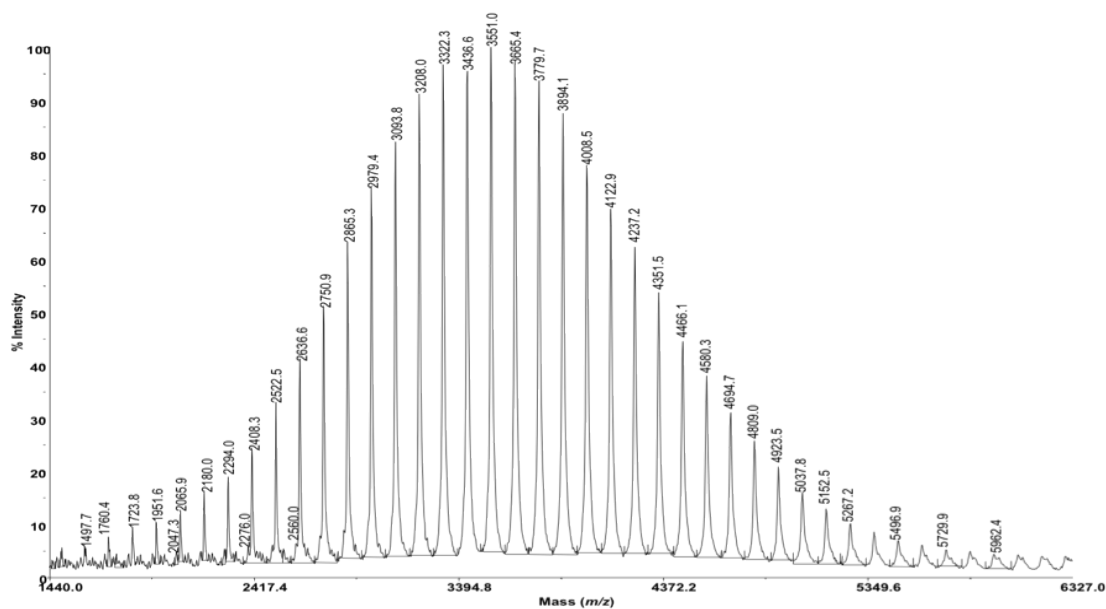


**Fig. S12** MALDI-TOF mass spectrum of PCL initiated by **3**-BnOH in toluene at 25 °C, [CL]/[**3**-BnOH] = 200 (Table 1, entry 24). The absolute mass values meet the data of  $114.14 \times n + 108$  for BnO-(CL)<sub>n</sub>-H,  $114.14 \times n + 108 + 17$  for BnO-(CL)<sub>n</sub>-OH and  $114.14 \times n + 108 + 17 + 22$  for BnO-(CL)<sub>n</sub>-OH·K<sup>+</sup>.

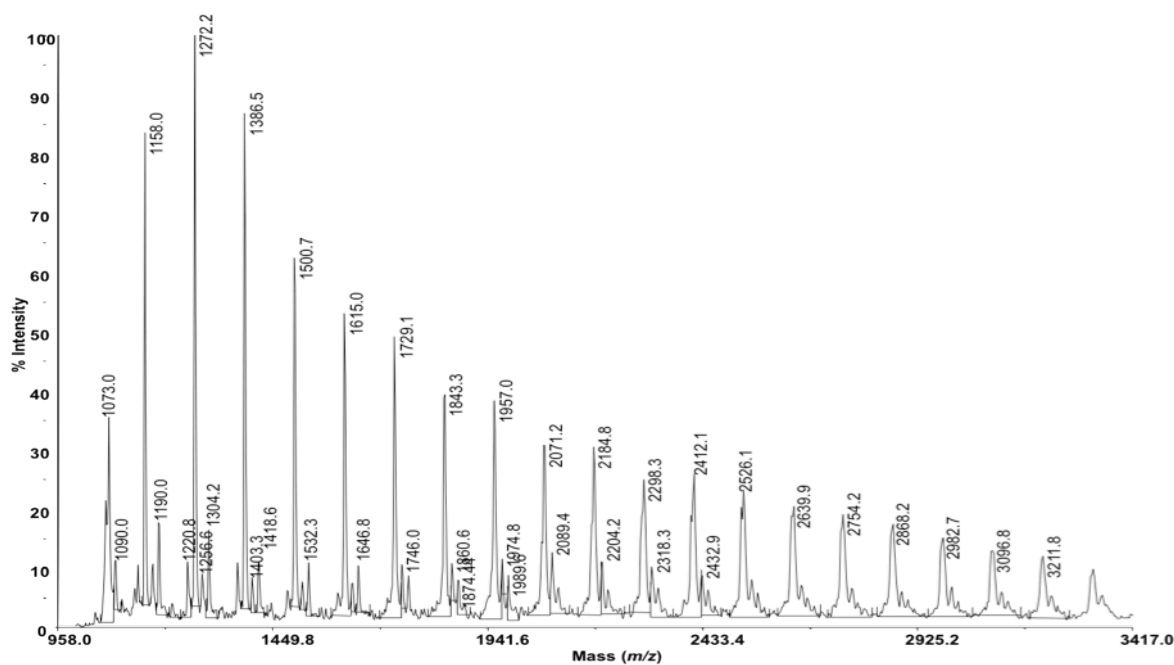


**Fig. S13** MALDI-TOF mass spectrum of PCL initiated by **3**-BnOH in toluene at 40 °C, [CL]/[**3**-BnOH] = 200 (Table 1, entry 20).

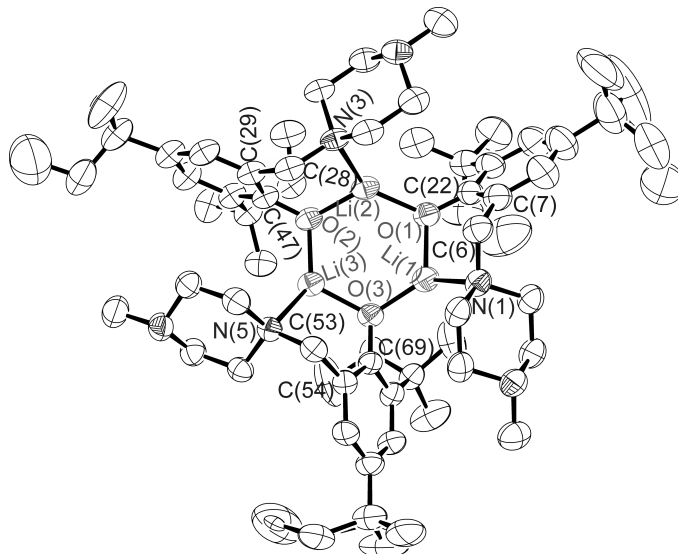


**Fig. S14** Molecular structure of **3**. (50% thermal ellipsoids; H atoms excluded for clarity). Selected bond lengths (Å) and bond angles (°): O(1)-Li(1), 1.839(5); O(1)-Li(2), 1.862(5); O(2)-Li(2), 1.839(5); O(2)-Li(3), 1.845(5); O(3)-Li(1), 1.837(5); O(3)-Li(3), 1.857(5); N(1)-Li(1), 2.133(5); N(3)-Li(2), 2.138(5); N(5)-Li(3), 2.150(6); Li(1)-O(1)-Li(2), 112.1(2); Li(2)-O(2)-Li(3), 115.5(2); Li(1)-O(3)-Li(3), 110.4(2); O(3)-Li(1)-O(1), 121.9(2); O(2)-Li(2)-O(1), 119.5(3); O(2)-Li(3)-O(3), 120.1(3); O(3)-Li(1)-N(1), 132.3(3); O(1)-Li(1)-N(1), 99.7(2); O(2)-Li(2)-N(3), 101.0(2).